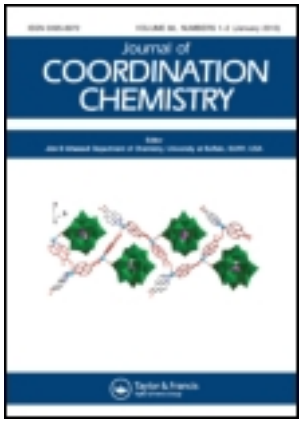

Journal of Coordination Chemistry
Publication details, including instructions for authors and subscription information:
http://www.tandfonline.com/loi/gcoo20

Synthesis and crystal structure of a new dicopper(II) complex with N-benzoato-N′-(hydroxypropyl)oxamide as ligand: cytotoxic activities and reactivities towards DNA and BSA

Xi-Ling Wang [a], Man Jiang [b], Yan-Tuan Li [a], Zhi-Yong Wu [a] & Cui-Wei Yan [c]

[a] Marine Drug & Food Institute, Ocean University of China, Qingdao, P.R. China

[b] Qindao Municipal Medical Group, Qindao, P.R. China

[c] College of Marine Life Science, Ocean University of China, Qingdao, P.R. China

Published online: 22 May 2013.

To cite this article: Xi-Ling Wang, Man Jiang, Yan-Tuan Li, Zhi-Yong Wu & Cui-Wei Yan (2013) Synthesis and crystal structure of a new dicopper(II) complex with N-benzoato-N′-(hydroxypropyl)oxamide as ligand: cytotoxic activities and reactivities towards DNA and BSA, Journal of Coordination Chemistry, 66:11, 1985-2003, DOI: 10.1080/00958972.2013.798732

To link to this article: http://dx.doi.org/10.1080/00958972.2013.798732

Journal of Coordination Chemistry, 2013
Vol. 66, No. 11, 1985–2003, http://dx.doi.org/10.1080/00958972.2013.798732

Synthesis and crystal structure of a new dicopper(II) complex with *N*-benzoato-*N*′-(hydroxypropyl)oxamide as ligand: cytotoxic activities and reactivities towards DNA and BSA

XI-LING WANG†, MAN JIANG‡, YAN-TUAN LI*†, ZHI-YONG WU† and CUI-WEI YAN*§

†Marine Drug & Food Institute, Ocean University of China, Qingdao, P.R. China
‡Qindao Municipal Medical Group, Qindao, P.R. China
§College of Marine Life Science, Ocean University of China, Qingdao, P.R. China

(*Received 8 January 2013; in final form 19 February 2013*)

A new dicopper(II) complex bridged by *N*-benzoato-*N*′-(hydroxypropyl)oxamide (H_3oxbpa) and end-capped with 1,10-phenanthroline (phen), $[Cu_2(oxbpa)(phen)(H_2O)](pic)\cdot 2H_2O$ (where pic denotes picrate anion) has been synthesized and characterized by elemental analyses, molar conductance, IR and electronic spectra studies, and single-crystal X-ray diffraction. In the crystal of the dicopper(II) complex, copper(II) ions are bridged by cis-oxamide with a Cu···Cu separation of 5.258(5) Å. The ones at the inner and the exo-sites of the cis-oxbpa^{3-} are square-planar and square-pyramidal coordination, respectively. These complexes are assembled to a one-dimensional chain via classical O–H···O hydrogen bonds. *In vitro* cytotoxicity shows that the dicopper(II) complex exhibits cytotoxic activity against SMMC7721 and A549 cell lines. The reactivity towards (Herring sperm DNA) and protein bovine serum albumin (BSA) revealed that the dicopper(II) complex can interact with DNA by intercalation, and the complex binds to protein BSA responsible for quenching of tryptophan fluorescence by static quenching mechanism.

Keywords: Crystal structure; Dicopper(II) complex; Oxamidato-bridge; *In vitro* anticancer activity; DNA interaction; Protein BSA binding

1. Introduction

The syntheses and interactions of transition metal complexes with DNA and protein have been an active field of research. Interest in this area is aimed at gaining insight into the mechanism involving site-specific recognition of DNA, the biochemical procedures governing protein sequencing, foot-printing and folding studies, understanding the reactive models for protein–nucleic acid interactions, application of probes of DNA structure, and obtaining information about the rational design and synthesis of new types of pharmaceutical molecules [1–3]. As a widely used metal-based antitumor drug targeting DNA, cisplatin is active in the treatment of several types of cancers [4, 5], but the side effects

*Corresponding author. Emails: yantuanli@ouc.edu.cn (Y.-T. Li); cuiweiyan@ouc.edu.cn (C.-W. Yan)

limit its potential efficacy [6]. The detailed molecular mechanism of its side effects has been elucidated, which involves covalent binding to DNA [7]. As a result, research has focused on more efficacious, target-specific, less toxic, and noncovalently DNA-binding cytotoxic drugs. Modes of DNA noncovalent interaction with metal complexes include electrostatic effect, groove binding, and intercalation. Among these noncovalent binding modes, intercalation is one of the most important DNA-binding modes, related to its various applications in cancer therapy and molecular biology [8]. Intercalating ability is not only related to planarity of ligands [9] but is also affected by metal ion type and valence, since these are responsible for the geometry of the complexes [10]. As attention has focused on developing metal-based therapeutics, there is interest in the analysis of drug–protein interactions that influence the absorption, distribution, metabolism, and excretion properties of drugs. As the most abundant proteins in the circulatory systems of a wide variety of organisms, serum albumins play an important role in transport and deposition of exogenous substances [11]. Among the serum albumins, bovine serum albumin (BSA) is an attractive macromolecule frequently used in biophysical and biochemical studies due to its structural homology with human serum albumin, its availability, low cost, and unusual ligand-binding properties [12]. Therefore, the reactivities of metal complexes towards DNA and BSA are useful in the design of small molecule anticancer therapeutics [13].

Many investigations have focused on the selection of metal ions and design of ligands. Metal complexes accelerate drug action and increase effectiveness of organic ligands [14] and medicinal properties of metal complexes depend on the nature of metal ions and ligands. Copper, with its bio-essential activity and oxidative nature, has attracted numerous studies of copper complexes with medical applications [15–17]. Particularly, copper complexes containing heterocyclic bases have been extensively explored for strong interactions with DNA and cytotoxic activities [18–21] since Sigman *et al.* first discovered that copper coordinated to 1,10-phenanthroline (phen) can cleave DNA [21]. Compared with the number of studies dealing with mononuclear complexes [21–23], relatively few studies on dinuclear complexes have been reported [24]. A number of proteins containing dinuclear metal centers play paramount roles in biology, including dioxygen transport or activation, electron transfer, reduction of nitrogen oxides, and hydrolytic chemistry, prompting us to design and synthesize new dinuclear complexes. In designing and synthesizing dinuclear systems, *N*,*N*′-bis(substituent)oxamides are good candidates in forming polynuclear complexes because their coordinating abilities toward transition metal ions can be modified by changing the nature of the amide substituents [25, 26]. Comparing with extensive research in symmetrical *N*,*N*′-bis(substituent)oxamide dinuclear complexes, only a few asymmetrical *N*,*N*′-bis(substituent)oxamide dinuclear complexes have been reported due to difficulties in their syntheses [27]. Exploration of the interactions of these complexes with DNA and protein BSA encourages us to synthesize new dicopper(II) complexes with asymmetrical *N*,*N*′-bis(substituted)oxamide bridging ligands, and phen as terminal ligand to evaluate the influence of asymmetrical *N*,*N*′-bis(substituted)oxamide bridging ligands on structure, DNA-binding properties and cytotoxic activities, and furthermore to gain some insight into the reactivity of this kind of complex towards protein BSA.

Taking into account the above facts, quite recently we reported the structures, anticancer activities, and DNA-binding properties of the dicopper(II) complex bridged by *N*-benzoato-*N*′-(2-amino-2-methylethyl)oxamide, and end-capping with phen [24]. As continuation of our ongoing program, in this paper, we describe the synthesis and structure of a new dicopper(II) complex, $[Cu_2(oxbpa)(phen)(H_2O)](pic)\cdot 2H_2O$, using *N*-benzoato-*N*′(hydroxypropyl)oxamide (H_3oxbpa) as a bridging ligand, and end-capped with phen. *In vitro*

cytotoxic activities and the reactivities towards DNA and protein BSA of the dicopper(II) complex have been studied. The results suggest that different bridging ligands in dinuclear complexes may play important roles in DNA- and BSA-binding properties and cytotoxic activities.

2. Experimental

2.1. *Materials and chemicals*

All reagents were AR grade and obtained commercially. The ligand *N*-benzoato-*N*′-(hydroxypropyl)oxamide (H_3oxbpa) and $Cu(pic)_2{\cdot}6H_2O$ were prepared according to literature methods [28, 29]. Doubly distilled water was used to prepare buffers. Ethidium bromide (EB), BSA, and herring sperm DNA (HS-DNA) were purchased from Sigma Corp.

2.2. *Physical measurements*

Carbon, hydrogen, and nitrogen analyses were performed with a Perkin–Elmer elemental analyzer Model 240. Molar conductance was measured with a Shanghai DDS-11A conductometer. The infrared spectrum was recorded with samples as KBr pellets in a Nicolet Impact 470 FTIR spectrophotometer from 4000 to 400 cm^{-1}. The UV–vis spectrum was recorded in a 1 cm path length quartz cell on a Cary 300 spectrophotometer. Fluorescence was tested on an Fp-750w fluorometer. A CHI 832 electrochemical analyzer (Shanghai CHI Instrument, Shanghai, China) with a glassy carbon working electrode (GCE), a saturated calomel reference electrode, and a platinum wire counter electrode were used for electrochemical measurements. The GCE surface was freshly polished to a mirror prior to each experiment with 0.05 μm α-Al_2O_3 paste and then cleaned in water for 5 min. Viscosity measurements were carried out using an Ubbelohde viscometer immersed in a thermostatic water bath maintained at 289 (±0.1) K.

2.3. *Synthesis of $[Cu_2(oxbpa)(phen)(H_2O)](pic){\cdot}2H_2O$*

A methanol aqueous solution (5 mL) of copper(II) picrate hexahydrate (0.0627 g, 0.1 mM) was added dropwise into a methanol solution (5 mL) containing H_3oxbpa (0.0133 g, 0.05 mM) and piperidine (0.0128 g, 0.15 mM). The mixture was stirred quickly for 30 min, then a methanol solution (5 mL) containing 1,10-phenanthroline (0.0099 g, 0.05 mM) was added. After the reaction system was stirred at 333 K for 6 h, the resulting dark green solution was filtered, and green cube crystals of the complex suitable for X-ray analysis were obtained by slow evaporation at room temperature after 10 days. Yield: 0.0303 g (71%). Anal. Calcd for $Cu_2C_{30}H_{27}N_7O_{15}$ (%): C, 42.26; H, 3.19; N, 11.50. Found (%): C, 42.24; H, 3.14; N, 11.51.

2.4. *Crystal structure determination*

The X-ray diffraction for the complex was carried out on a Bruker APEX area-detector diffractometer with graphite monochromatic Mo-Kα radiation ($\kappa = 0.71073$ Å) at 296 K. The crystal structure was solved by direct methods followed by Fourier syntheses. Structure refinement was performed by full matrix least-squares procedures using SHELXL-97 on

Table 1. Crystal data and details of the structure determination for the complex.

Empirical formula	$Cu_2C_{30}H_{27}N_7O_{15}$
Formula weight	852.67
Crystal system	Triclinic
Space group	$P-1$
a (Å)	8.347(12)
b (Å)	16.23(2)
c (Å)	13.57(2)
α	108.56(2)
β (°)	82.60(3)
γ (°)	103.36(2)
V (Å^3)	1693(4)
Z	2
D (Calcd) (g cm^{-3})	1.673
μ (Mo-Kα) (mm^{-1})	1.341
F(000)	868
Crystal size (mm)	$0.09 \times 0.11 \times 0.25$
Temperature (K)	296(2)
Radiation (Å)	Mo-Kα 0.71073
θ range for data collection (°)	2.37–26.15
Tot., Uniq. data, R(int)	8915, 6601, 0.035
Observed data [$I > 2\sigma(I)$]	3719
R, ωR_2, S	0.0689, 0.1861, 0.961
Max., av. shift/error	0.001, 0.000

Table 2. Selected bond distances (Å) and angles (°) for the complex.

Cu1–N1	1.991(6)	Cu1–N2	1.938(6)
Cu1–O1	1.904(5)	Cu1–O5	1.990(5)
Cu2–N3	2.027(6)	Cu2–N4	2.007(5)
Cu2–O3	1.996(5)	Cu2–O4	1.969(5)
Cu2–O6	2.336(6)	–	–
O1–Cu1–O5	87.0(2)	O1–Cu1–N1	94.41(19)
O1–Cu1–N2	175.4(2)	O5–Cu1–N1	177.3(2)
O5–Cu1–N2	92.7(2)	N1–Cu1–N2	86.1(2)
O3–Cu2–O4	83.93(18)	O3–Cu2–O6	95.8(2)
O3–Cu2–N3	97.7(2)	O3–Cu2–N4	168.6(2)
O4–Cu2–O6	92.0(2)	O4–Cu2–N3	173.3(2)
O4–Cu2–N4	93.63(19)	O6–Cu2–N3	94.2(2)
O6–Cu2–N4	95.4(2)	N3–Cu2–N4	83.5(2)

F^2 [30]. Two carbons of hydroxypropylamine arm of oxbpa^{3-} are disordered at two parts (C11A, C12A, and C11B, C12B) with refined occupancies of 0.77(2) and 0.23(2), respectively. The hydrogens on carbons were placed in calculated positions with C–H = 0.93 (aromatic) and 0.97 Å (methylene) then refined in a riding mode, with Uiso(H) = 1.2 Ueq(C atoms). The water hydrogens were found in a difference Fourier map and treated as riding with Uiso(H) = 1.5 Ueq(O atoms). The hydroxyl H was located in a difference Fourier map and refined freely. Crystal data and structural refinement parameters are summarized in table 1, and selected bond distances and angles are listed in table 2.

2.5. *DNA interaction studies*

All experiments involving HS-DNA were performed in *tris*(hydroxymethyl)aminomethane–HCl (*Tris*–HCl) buffer solution (pH 7.16), which was prepared using deionized and sonicated triply distilled water. Solution of DNA in *Tris*–HCl buffer gave ratio of UV

absorbance at 260 and 280 nm, A_{260}/A_{280}, of *ca.* 1.9, indicating that the DNA was sufficiently free of protein [31]. The concentration of the prepared DNA stock solution was determined according to its absorbance at 260 nm. The molar absorption coefficient, ε_{260}, was taken as 6600 L M^{-1} cm^{-1} [32]. Stock solution of DNA was stored at 277 K and used after no more than four days. Concentrated stock solution of the dicopper(II) complex was prepared by dissolving the complex in DMSO and diluting with *Tris*–HCl buffer to required concentrations for all the experiments. Absorption spectral titration experiment was performed by keeping the concentration of the dicopper(II) complex constant while varying the HS-DNA concentration. Equal solution of HS-DNA was added to the copper (II) complex solution and reference solution to eliminate the absorbance of HS-DNA itself. In the EB fluorescence displacement experiment, 5 μL of EB *Tris*–HCl solution (1 mM L^{-1}) was added to 1 mL of HS-DNA solution (at saturated binding levels) [33] and stored in the dark for 2 h. Then the solution of the copper(II) complex was titrated into the DNA/EB mixture and diluted in *Tris*–HCl buffer to 5 mL. Before taking measurements, the mixture was shaken and incubated at room temperature for 30 min. The fluorescence spectra of EB bound to HS-DNA were obtained at an emission wavelength of 584 nm in the fluorometer, keeping the concentration of HS-DNA constant while varying the concentration of the complex. The electrochemical titration experiment was also performed by keeping the concentration of the complex constant while varying HS-DNA concentration, using a solvent of 50 mM NaCl/5 mM *Tris*–HCl buffer solution at pH 7.16 [34]. All voltammetric experiments were performed in a single compartment cell. The supporting electrolyte was 50 mM NaCl/5 mM *Tris*–HCl buffer solution at pH 7.16 [34]. The solutions were deoxygenated by purging with nitrogen for 15 min prior to measurements; during measurements a stream of N_2 was passed over the solution. In viscosity measurements, a HS-DNA sample approximately 200 base pairs in length was prepared by sonication in order to minimize complexities arising from DNA flexibility [35]. Flow times were measured with a digital stopwatch, and each sample was measured three times, and an average flow time was calculated. Relative viscosities for HS-DNA in the presence and absence of the complex were calculated from the relation $\eta = (t - t_0)/t_0$, where t is the observed flow time of DNA-containing solution and t_0 is that of *Tris*–HCl buffer alone. Data were presented as $(\eta/\eta_0)^{1/3}$ *versus* binding ratio [36], where η is the viscosity of DNA in the presence of the complex and η_0 is the viscosity of DNA alone.

2.6. *BSA binding studies*

All experiments involving BSA were performed in 50 mM NaCl/Tris–HCl buffer solution (pH 7.16). Solutions of BSA and the dicopper(II) complex were prepared by dissolving them in the NaCl/Tris–HCl buffer solution to the required concentrations. For UV absorption experiment, a 5 mL solution of BSA (10 μM) was titrated and the BSA concentration is kept constant while varying the concentration of the complex. An equal solution of the complex was added to the reference solution to eliminate the absorbance of the complex itself. In the tryptophan fluorescence quenching experiment, quenching of the tryptophan residues of BSA [37] was done by keeping the concentration of the BSA constant while varying the complex (quencher) concentration, producing solutions with varied mole ratio of the quencher to BSA. Fluorescence spectra were recorded at an excitation wavelength of 295 nm and an emission wavelength of 347 nm in the fluorometer after each addition of the quencher.

2.7. *In vitro antitumor activity evaluation by SRB assays*

The cytotoxicities of the dicopper(II) complex were evaluated against SMMC-7721 and A549 cancer cell lines by using the sulforhodamine B (SRB) assay. All cells were cultured in RPMI 1640 supplemented with 10% (v/v) fetal bovine serum, 1% (w/v) penicillin ($104\,U\,mL^{-1}$) and $10\,mg\,mL^{-1}$ streptomycin. Cell lines are maintained at 310 K in a 5% (v/v) CO_2 atmosphere with 95% (v/v) humidity. Cultures were passaged weekly using trypsin–EDTA to detach the cells from their culture flasks. The dicopper(II) complex was dissolved in DMSO and diluted to the required concentration with culture medium when used. The content of DMSO in the final concentrations did not exceed 0.1%. At this concentration, DMSO was found to be non-toxic to the cells tested. Rapidly growing cells were harvested, counted, and incubated at the appropriate concentration in 96 well microplates for 24 h. The dicopper(II) complex dissolved in culture medium was then applied to the culture wells to achieve final concentrations ranging from 10^{-4} to $10^{-1}\,\mu M$. Control wells were prepared by the addition of culture medium without cells. The plates were incubated at 310 K in a 5% CO_2 atmosphere for 48 h. Upon completion of the incubation, the cells were fixed with ice cold 10% trichloroacetic acid (100 mL) for 1 h at 277 K, washed five times in distilled water and allowed to dry in air and stained with 0.4% SRB in 1% acetic acid (100 mL) for 15 min. The cells were washed four times in 1% acetic acid and airdried. The stain was solubilized in 10 mM unbuffered Tris base (100 mL) and the OD of each well was measured at 540 nm on a microplate spectrophotometer. The IC_{50} values were calculated from curves constructed by plotting cell survival (%) *versus* the dicopper(II) complex and concentration ($\mu g\,mL^{-1}$).

3. Results and discussion

3.1. *Synthetic route of the dicopper(II) complex*

Our aim was to obtain dicopper(II) complex, therefore, *N*-benzoato-*N′*-(hydroxyl-propyl) oxamide (H_3oxbpa), which can coordinate to metal ions through carbonyl oxygens and nitrogens of the oxamido, was chosen as the bridging ligand; 1,10-phenanthroline (phen) was used as the terminal ligand. In preparing the complex, piperidine as base makes the bridging ligand (H_3oxbpa) coordinate to copper(II) through deprotonated oxamido nitrogen and carbonyl oxygens. Elemental analyses indicate that the reaction of H_3oxbpa with $Cu(pic)_2{\cdot}6H_2O$ and phen in 1 : 2 : 1 M ratio yielded the dinuclear $[Cu_2(oxbpa)(phen)(H_2O)](pic){\cdot}2H_2O$, as expected. The synthetic pathway for the complex may be represented by scheme 1.

3.2. *General property of the dicopper(II) complex*

The dicopper(II) complex is insoluble in non-polar solvents and common polar solvents, moderately soluble in methanol and acetonitrile, and very soluble in DMF and DMSO to give stable solutions at room temperature. In the solid state, the dicopper(II) complex is fairly stable in air allowing physical measurements. For the dicopper(II) complex, the molar conductance value ($76\ \Omega^{-1}\,cm^2\,M^{-1}$) in DMF falls in the expected range for 1 : 1 electrolyte [38], suggesting that the dicopper(II) complex consists of a dicopper(II) complex cation $[Cu_2(oxbpa)(phen)(H_2O)]^+$ and an uncoordinated picrate in solution. The observation coincides with the following spectral characterization.

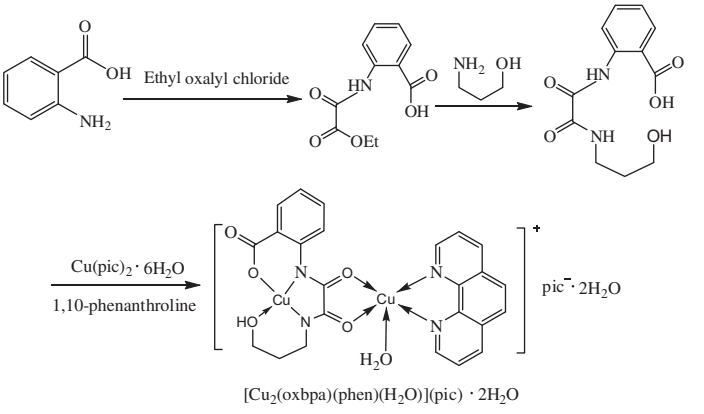

Scheme 1. The synthetic pathway for the binuclear copper(II) complex.

3.3. *IR spectra*

IR spectrum in the range 4000–400 cm^{-1} is studied in comparison with that of the free H_3oxbpa. The carbonyl (C=O) stretch of H_3oxbpa (1662 cm^{-1}) shifts to 1633 cm^{-1} in the IR spectrum of the complex. This shift has often been used as a diagnostic indicator for oxamido-bridged structure [39]. The –C=N– stretch for aromatic rings of phen shift to higher frequency, 1567 cm^{-1}, indicating coordination in the dicopper(II) complex. There are $\nu_s(NO_2)$ at 1342 cm^{-1} and $\nu_{as}(NO_2)$ at 1555 cm^{-1} in uncoordinated 2,4,6-trinitrophenol (Hpic). However, in the dicopper(II) complex, $\nu_s(NO_2)$ of pic splits into two bands at 1332 and 1361 cm^{-1}, and $\nu_{as}(NO_2)$ of pic emerges at 1519 cm^{-1}, suggesting that the nitryl oxygens of pic take no part in coordination [24], consistent with the molar conductance measurement and crystal structure of the dicopper(II) complex (*vide infra*).

3.4. *Electronic spectra*

The electronic spectrum of the dicopper(II) complex was measured from 200 to 800 nm. Spectra at different concentrations (1.2×10^{-5}–1.2×10^{-6} M) obeyed the Beer–Lambert law, indicating that the dicopper(II) complex stays intact at these concentrations [40]. Three main absorptions with varied intensities can be observed. The intense band at 235 nm is assigned to inter- or intra-ligand (π–π^*) transition, while the band at 272 nm in the complex can be assigned to the charge transfer transition between the ligand and metal. A broad band with low absorptivity is observed at 602 nm in the spectrum, corresponding to the d–d transition of copper(II) [28].

These spectroscopic data of the dicopper(II) complex are in accord with the crystal structure.

3.5. *Structure description of $[Cu_2(oxbpa)(phen)(H_2O)](pic)\cdot 2H_2O$*

The complex consists of a dicopper(II) cation $[Cu_2(oxbpa)(phen)(H_2O)]^+$, a picrate anion, and two lattice waters as illustrated in figure 1 and in which two copper(II) ions are bridged by cis-oxbpa^{3-} with a Cu···Cu distance of 5.258(5) Å. The *cis*-oxamide group coordinates to Cu1 and Cu2 in the usual chelating mode, with bite angles of 86.1(2)° and 83.93(18)°, respectively. The inner Cu1 has a square planar coordination geometry with

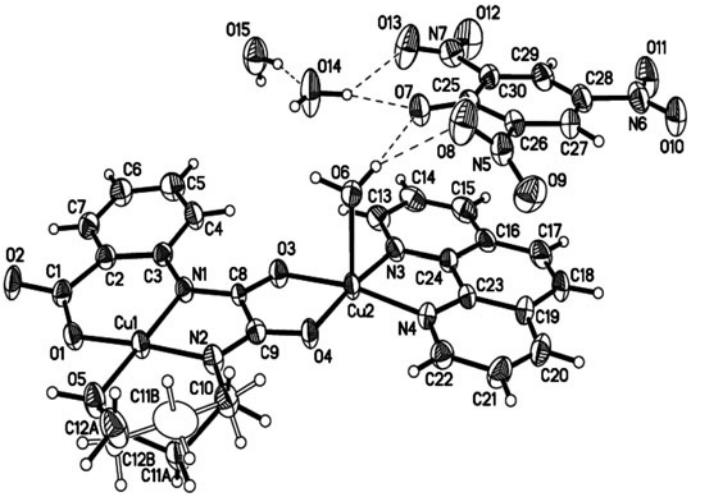

Figure 1. A view of the complex with the atom numbering scheme. Displacement ellipsoids are drawn at 30% probability and hydrogens are shown as small spheres of arbitrary radii. Dashed lines show hydrogen bonds.

deviation of 0.018(3) Å from the coordination plane of the defined atoms (0.060(3) Å). Cu1 has three chelating rings, in which the six-membered hydroxypropylamine arm is disordered and adopts conformation between the half-chair and envelope. The exo Cu2 is located in a square pyramidal environment with τ of 0.08 [41]. The basal plane is defined by two exo-oxygens of $oxbpa^{3-}$ and two nitrogens from phen. The apical site is occupied by a water (O6), by which Cu2 is pulled 0.153(3) Å out of the basal plane.

In the crystal, four solvent waters and two pic build up a cyclic hydrogen bonding system. Two $[Cu_2(oxbpa)(phen)(H_2O)]^+$ link through hydrogen bonds between the coordination waters (O6) and the carboxyl oxygens (O2) to form a dimer. As illustrated in figure 2, the two kinds of components (table 3) are sequentially assembled into a 1-D chain parallel to the *b* axis.

3.6. *In vitro antitumor activities of the complex*

In vitro antitumor activities of the dicopper(II) complex and cisplatin against two cancer cell lines, human hepatocellular carcinoma cell line SMMC-7721 and human lung adenocarcinoma cell line A549 were conducted in our study. The IC_{50} values of the present dicopper(II) complex for the SMMC-7721 and A549 cell lines are 10.2 ± 0.7 and $13.5 \pm 0.8\,\mu g\,mL^{-1}$, respectively, lower than those of an analogous dicopper(II) complex $[Cu_2(oxbm)(phen)(H_2O)(CH_3OH)](pic)$ (SMMC-7721, $13 \pm 0.7\,\mu g\,mL^{-1}$; A549, $16 \pm 0.8\,\mu g\,mL^{-1}$) [24], indicating that the present dicopper(II) complex has better activities than the previously reported dicopper(II) complex. The order of *in vitro* anticancer activities for the two dicopper (II) complexes is consistent with their DNA-binding abilities (*vide infra*). The *in vitro* cytotoxicities for the two dicopper(II) complexes are less than those of cisplatin (IC_{50} values are 5.4 ± 0.2 and $7.6 \pm 0.4\,ng\,mL^{-1}$ for these two kinds of cancer cell lines), but the inhibition of cell proliferation produced by the two dicopper(II) complexes on the same batch of cell lines is still significant, implying that these dicopper(II) complexes may have applications for the development of nucleic acid molecular probes and new therapeutic reagents for diseases.

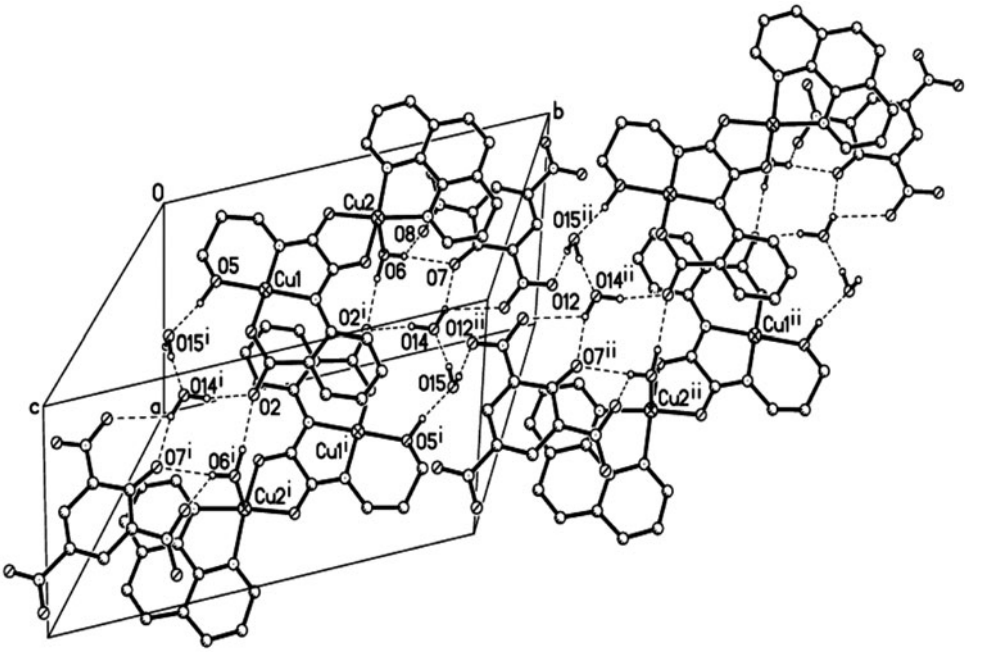

Figure 2. A 1-D hydrogen-bonding structure parallel to the *b*-axis. Hydrogen bonds are shown as dotted lines; hydrogens uninvolved have been omitted for clarity (symmetry codes: (i) $1-x$, $1-y$, $1-z$; (ii) $1-x$, $2-y$, $1-z$).

Table 3. Hydrogen-bonding geometries for the complex (Å, °).

D–H···A	D–H	H···A	D···A	D–H···A
O5–H5···O15^{i}	0.97(7)	1.65(7)	2.607(8)	170(6)
O6–H6A···O2^{i}	0.92	1.88	2.795(7)	170.4
O6–H6B···O7	0.87	2.10	2.944(8)	162.1
O6–H6B···O8	0.87	2.54	3.124(9)	124.9
O14–H14A···O2^{i}	0.96	1.86	2.798(9)	167.1
O14–H14B···O7	0.92	1.97	2.851(8)	161.8
O14–H14B···O13	0.92	2.42	3.009(10)	122.5
O15–H15A···O14	0.91	1.66	2.550(9)	166.7
O15–H15B···O12^{ii}	0.87	2.15	3.014(11)	172.4

Symmetry codes: (i) $1-x$, $1-y$, $1-z$; (ii) $1-x$, $2-y$, $1-z$.

These findings of cytotoxic activities *in vitro* of the dicopper(II) complex prompt us to further explore the reactivities towards DNA and protein BSA.

3.7. *DNA interaction studies*

3.7.1. Electronic absorption titration. Electronic absorption spectroscopy is an effective method to examine binding modes and binding extent of metal complexes with DNA. Binding with DNA through intercalation usually results in hypochromism and bathochromism, due to strong stacking interaction between an aromatic chromophore and the base

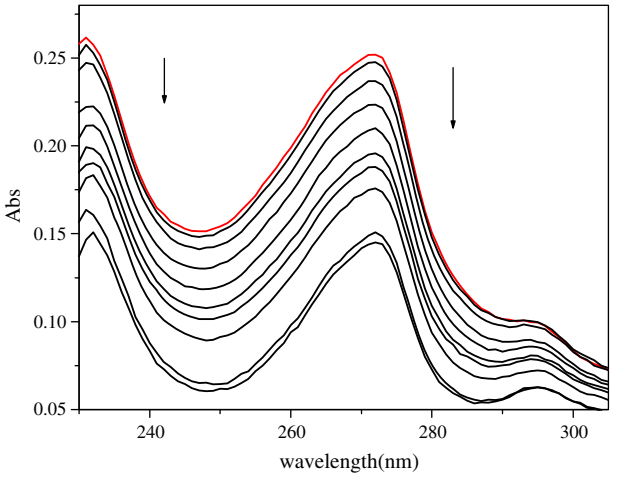

Figure 3. Absorption spectra of complex upon titration of HS-DNA. Arrows indicate the change upon increasing DNA concentration (the red line for the absence of HS-DNA) (see http://dx.doi.org/10.1080/00958972.2013.798732 for color version).

pairs of DNA [42]. Absorption titration of the dicopper(II) complex was performed using a fixed dicopper(II) complex concentration to which increments of HS-DNA stock solution were added. The absorption spectra of the dicopper(II) complex in the absence and presence of DNA are given in figure 3. When titrated by HS-DNA, the transition band of the dicopper(II) complex at 272 nm exhibits hypochromism of about 22.2% with 4 nm red shift at a ratio of [DNA]/[complex] of 8. These spectral characteristics suggest that the dicopper (II) complex interacts with HS-DNA through intercalation. When the dicopper(II) complex intercalates in the base pairs of HS-DNA, the π^*-orbital of the intercalated ligand (phen) in the complex can couple with the π-orbital of the base pairs of HS-DNA, thus decreasing the π–π^* transition energy and leading to the bathochromism. The coupling π-orbital is partially occupied by electrons, thus decreasing the transition probabilities and resulting in hypochromism.

To evaluate quantitatively the affinity of the dicopper(II) complex towards HS-DNA, the intrinsic binding constant K_b was determined by monitoring the changes in absorbance at 272 nm for the dicopper(II) complex using the following equation [42]:

$$[\mathrm{DNA}]/(\varepsilon_a - \varepsilon_f) = [\mathrm{DNA}]/(\varepsilon_b - \varepsilon_f) + 1/K_b(\varepsilon_a - \varepsilon_f) \quad (1)$$

where [DNA] is the concentration of HS-DNA, ε_a, ε_f and ε_b correspond to the extinction coefficients, for each addition of HS-DNA to the dicopper(II) complex, for the free dicopper(II) complex and for the dicopper(II) complex in the fully bound form, respectively. From the plot of $[\mathrm{DNA}]/(\varepsilon_a - \varepsilon_f)$ *versus* [DNA], illustrated in figure 4, the binding constant K_b is given by the ratio of the slope to the intercept. The intrinsic binding constant K_b for the dicopper(II) complex is $1.50 \times 10^5\,\mathrm{M}^{-1}$ ($R = 0.9952$ for seven points). The K_b value is lower than that observed for a classical intercalator (e.g. EB-DNA, $\sim 10^6\,\mathrm{M}^{-1}$) [43], and has the same level as that of the DNA-intercalative dicopper(II) complex [44], but higher than those of mononuclear copper(II) complexes [22, 45, 46] and 1-D polymeric copper (II) complexes [47, 48], indicating that the present dicopper(II) complex can strongly bind to HS-DNA by intercalation. The better binding affinity of the present dicopper(II)

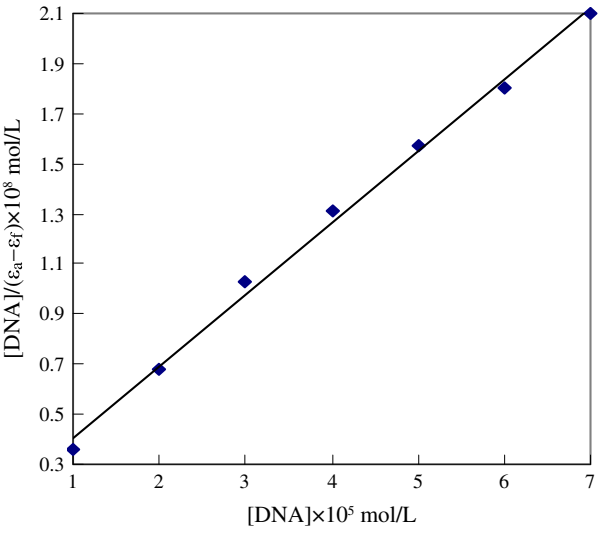

Figure 4. Plot of $[DNA]/(\varepsilon_a - \varepsilon_f)$ *vs.* [DNA] for absorption titration of HS-DNA with the complex.

complex may be due to the extended aromaticity and coplanarity of the phenanthroline ring system for better stacking between the base pairs of DNA, as well as the oxamido-bridge ligand [28].

3.7.2. Fluorescence titration. The competitive binding experiment was employed to clarify the binding mode of the dicopper(II) complex with HS-DNA. In general, the fluorescence intensity of DNA or EB in Tris buffer is very low. However, EB, which is one of the most sensitive fluorescence probes, emits intense fluorescence in the presence of DNA due to its strong intercalation between adjacent DNA base pairs [49] and this enhanced fluorescence could be quenched by addition of another molecule [50] owing to the decreasing binding sites of the DNA available for EB [50, 51]. Thus, EB can be used to probe the interaction of complexes with DNA. The emission spectra of EB bound to HS-DNA in the absence and presence of dicopper(II) complex are shown in figure 5. For the dicopper(II) complex the fluorescence intensity of EB-DNA at 584 nm exhibits a remarkable decrease with increasing concentration of the dicopper(II) complex, suggesting that some EB molecules were released after exchange with the dicopper(II) complex, resulting in fluorescence quenching of EB. This observation is often the characteristic of intercalation and coincides with other intercalators [52]. The quenching of EB bound to HS-DNA by the dicopper(II) complex is in agreement with the linear Stern–Volmer equation [53]:

$$I_0/I = 1 + K_{sv}[Q] \tag{2}$$

where I_0 and I represent fluorescence intensities in the absence and presence of quencher, respectively, K_{sv} is the Stern–Volmer constant, and $[Q]$ is the concentration of quencher. In the quenching plot of I_0/I *versus* [complex] (figure 6), K_{sv} of the dicopper(II) complex is given by the ratio of the slope to intercept as 9.43×10^4 ($R = 0.9940$ for nine points).

Comparing K_b and K_{sv} values of $[Cu_2(oxbpa)(phen)(H_2O)](pic)\cdot 2H_2O$ (K_b, $1.50 \times 10^5\,M^{-1}$; K_{sv}, 9.43×10^4) with those of its analogous dicopper(II) complex

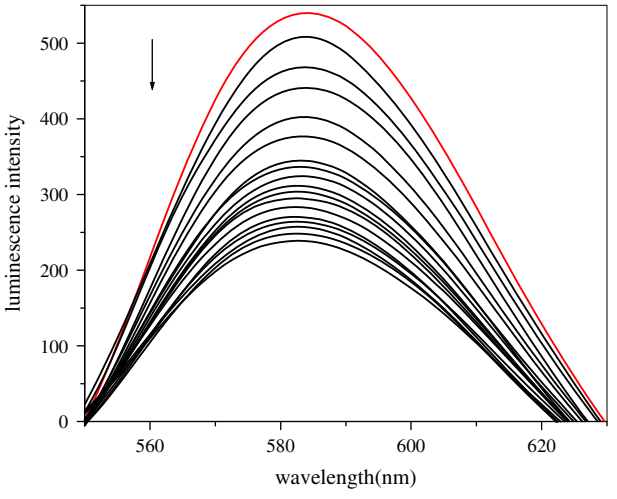

Figure 5. Fluorescence intensity of EB-DNA as the system was titrated with the complex. Arrow shows the direction of change upon increasing the complex concentration.

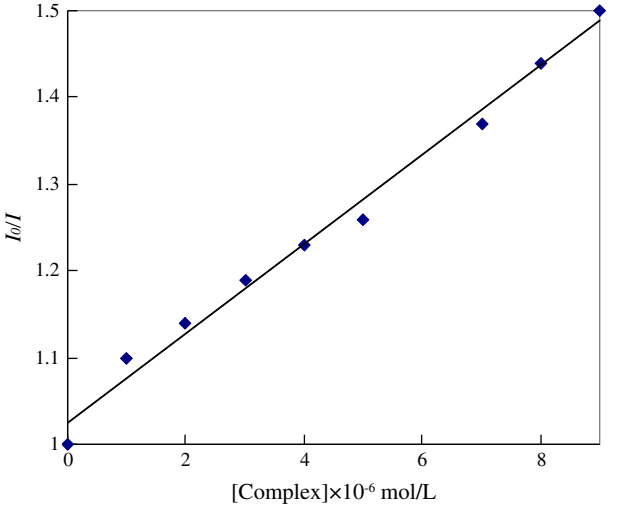

Figure 6. Plot of I_0/I *vs.* [complex] for the absorption titration of the complex.

$[Cu_2(oxbm)(phen)(H_2O)(CH_3OH)](pic)$ (K_b, $2.25 \times 10^4\,M^{-1}$; K_{sv}, 2.19×10^4) [24] [H_3oxbm is *N*-benzoato-*N*′-(2-amino-2-methylethyl)oxamido], we find that the K_b and K_{sv} values of the former are both higher than those of the latter, implying that the different oxamidato-bridge ligands have significant effects on both molecular and electronic structure. The large methyl in H_3oxbm of the previously reported dicopper(II) complex results in increasing steric hindrance, when the dicopper(II) complex intercalates into HS-DNA. Methyl, as an electron pushing group, will increase the electron density on the intercalating ligands, hence reinforcing the repulsion between the complex and DNA with the negatively charged phosphate backbone, and consequently destabilize the DNA-complex system, causing a decrease in the DNA-binding affinity. These results reveal that the affinity of the

two dicopper(II) complexes toward HS-DNA may be modified by changing the oxamidato-bridge ligands.

We also compared the DNA-binding properties of the present dicopper(II) complex with those of our previously reported polycopper(II) complexes with *N*,*N*′-bis(substituted)oxamides as bridging ligands and polypyridines as terminal ligands [28, 48, 54, 55, 57], and we find that not only the interaction modes but also the DNA-binding ability of these μ-oxamido-bridged polynuclear complexes are different, suggesting that interactions of this class of complexes towards HS-DNA may be tuned by changing the bridging or terminal ligands. Such strategy should be valuable in designing new μ-oxamido-bridged polynuclear complexes and understanding the binding between oxamido complexes and DNA. Further investigations are in progress using various bridging and terminal ligands to confirm the effect and gain deeper insights into this exciting field of DNA interactions.

3.7.3. Electrochemical titration. Cyclic Voltammetry (CV) provides a useful complement to the previously used methods of investigating binding of metal complexes to DNA [56]. The CV behaviors of the dicopper(II) complex without and with HS-DNA are shown in figure 7. In the absence of HS-DNA (red line), the dicopper(II) complex shows a quasi-reversible redox process corresponding to Cu(II)/Cu(I) with the cathodic (E_{pc}) and anodic peak potential (E_{pa}) being −0.211 and −0.071 V. The formal potential of the Cu(I)/Cu(II) couple in free form (E_f^o), taken as the average of E_{pc} and E_{pa}, is −0.141 V. In the presence of HS-DNA (blue line) with [DNA]/[complex] = 4 the voltammetric peak currents decreased, indicating interactions between the dicopper(II) complex and HS-DNA [56]. The drop of the voltammetric current in the presence of HS-DNA may be attributed to slow diffusion of the dicopper(II) complex bound to HS-DNA. The cathodic and anodic peak potentials are −0.201 and −0.054 V for the dicopper(II) complex. The formal potential of the Cu(I)/Cu(II) couple in binding form (E_b^o) is −0.128 V, shifted positive by 0.013 V, indicating that the dicopper(II) complex binds intercalatively to HS-DNA [57].

The separation between $E_b^{o\prime}$ and $E_f^{o\prime}$ can be used to estimate the ratio of binding constants for the reduced and oxidized forms to DNA using the equation [58]:

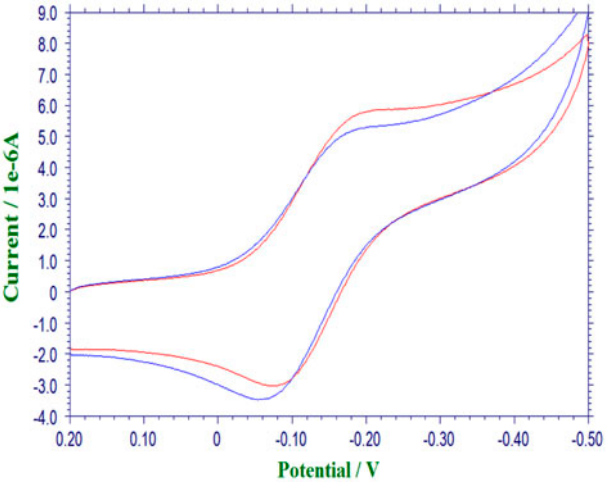

Figure 7. Cyclic voltammograms of the complex in the absence (red line) and presence (blue line) of HS-DNA (see http://dx.doi.org/10.1080/00958972.2013.798732 for color version).

$$\Delta E^{o'} = E_b^{o'} - E_f^{o'} = 0.059 \log(K_R/K_O) \quad (3)$$

where K_R and K_O are the binding constants of Cu(I) and Cu(II) to DNA, respectively. The ratio of constants for the binding of Cu(I) and Cu(II) to HS-DNA is estimated to be 1.66 for the dicopper(II) complex, intimating that the reduced form of the complex interacts more strongly than the oxidized one. These results are consistent with the above spectral observations.

3.7.4. Viscosity measurements. To further confirm the interaction mode of the dicopper (II) complex with HS-DNA, viscosity measurements were carried out. In classical intercalation the DNA helix lengthens as base pairs are separated to accommodate the bound ligand leading to increased DNA viscosity, whereas a partial, non-classical intercalation causes a bend in DNA helix reducing its effective length and thereby its viscosity. Viscosity measurement is regarded as the least ambiguous and the most critical means of investigating the binding mode of metal complexes with DNA in solution and provides strong arguments for intercalative binding [59, 60]. As shown in figure 8, the relative viscosity of HS-DNA increased with increasing concentration of the dicopper(II) complex, proving that the dicopper(II) complex binds to HS-DNA by intercalation. Thus, the results obtained from viscosity studies validate those obtained from spectral and electrochemical titrations.

3.8. *BSA-binding properties*

3.8.1. UV absorption spectra of BSA in the presence of the dicopper(II) complex. The binding of the dicopper(II) complex with protein BSA is explored by UV absorption spectra, and the results are shown in figure 9. Free BSA has maximum absorption at

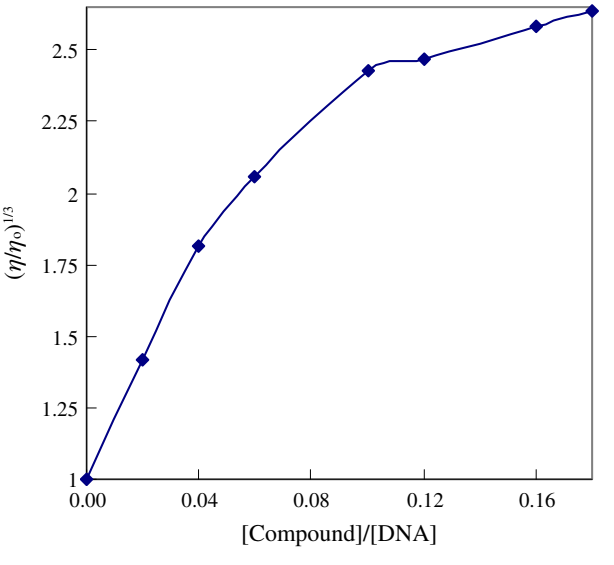

Figure 8. Effects of the increasing amount of the complex on the relative viscosity of HS-DNA at 289 (±0.1) K.

278 nm and increases with the addition of the dicopper(II) complex. This indicates interaction of BSA with the dicopper(II) complex [61].

3.8.2. Tryptophan quenching experiment. Binding of metal complexes to BSA can be detected by examining fluorescence spectra. Fluorescence of protein is caused by three intrinsic characteristics of the protein, tryptophan, tyrosine, and phenyl alanine residues. The intrinsic fluorescence of many proteins is mainly contributed by tryptophan alone. Fluorescence quenching refers to any process which causes a decrease of the fluorescence intensity from a fluorophore due to a variety of molecular interactions. These include excited-state reactions, molecular rearrangements, energy transfer ground-state complex formation, and collisional quenching. Quenching occurs by different mechanisms, which are usually classified as dynamic quenching and static quenching; dynamic quenching refers to a process in which the fluorophore and the quencher come into contact during the transient existence of the excited state. Static quenching refers to fluorophore-quencher complex formation. In both cases, the fluorescence intensity is related to the concentration of the quencher. Therefore, the quenched fluorophore serves as an indicator for quenching agent. In our experiment, shown in figure 10, the fluorescence emission intensity of BSA at 345 nm shows a remarkable decrease with increasing concentration of the dicopper(II) complex, indicating that the interaction of dicopper(II) complex with BSA causes some changes in protein secondary structure leading to changes in tryptophan environment of BSA [62].

To understand quantitatively the magnitude of the dicopper(II) complex quenching emission intensity of BSA, the linear Stern–Volmer equation is employed:

$$I_0/I = 1 + K_{sv}[Q] = 1 + K_q\tau_0[Q] \tag{4}$$

where I_0 and I represent the fluorescence intensities in the absence and presence of quencher, respectively. Q is the concentration of quencher and K_{sv} is a linear Stern–Volmer

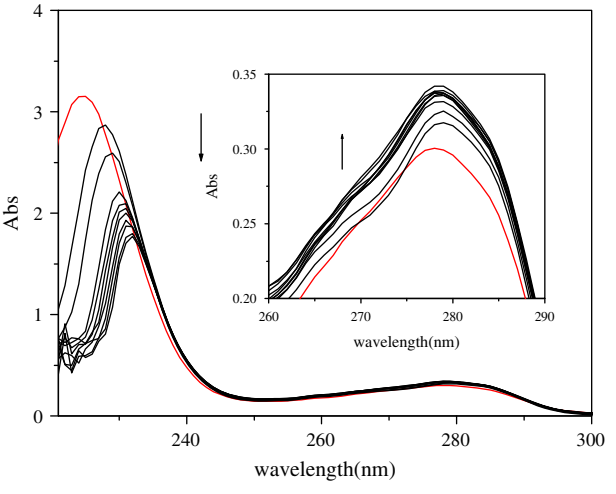

Figure 9. Absorption spectra of BSA upon titration of the complex. Arrow indicates the change upon increasing the complex concentration.

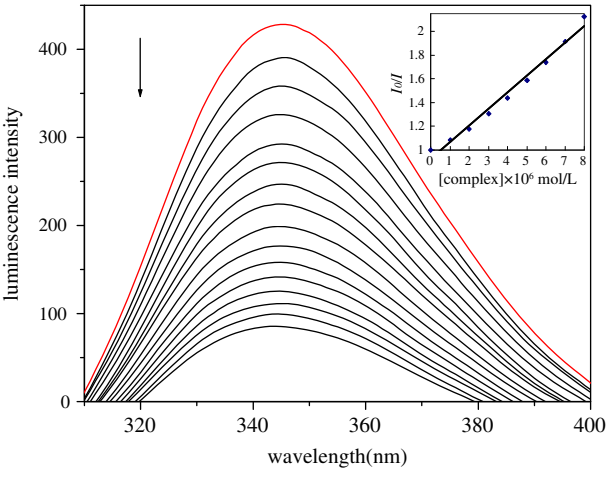

Figure 10. Emission spectra of BSA upon titration of the complex. Arrow shows the change upon the increasing complex concentration. Inset: Plot of I_0/I *vs.* [complex] for titration of the complex to BSA.

quenching constant. K_q is the bimolecular quenching rate constant, τ_0 is the average lifetime of the fluorophore in absence of the quencher as 10^{-8} s. From the quenching plot of I_0/I *versus* [complex] (inset in figure 10), K_q and K_{sv} of the dicopper(II) complex obtained from the slope are $1.50 \times 10^{13}\,M^{-1}\,s^{-1}$ and $1.50 \times 10^{5}\,M^{-1}$, respectively. K_q is greater than the maximum collision quenching constant of various kinds of quenchers to biomacromolecule being $2.0 \times 10^{10}\,M^{-1}\,s^{-1}$ [63], showing that the above quenching is not initiated by dynamic collision but via the combination of the dicopper(II) complex and BSA. Therefore, the quenching of BSA fluorescence by the dicopper(II) complex depends on formation of the complex between dicopper(II) complex and BSA. The binding constant (K) was calculated by the method given in the following section.

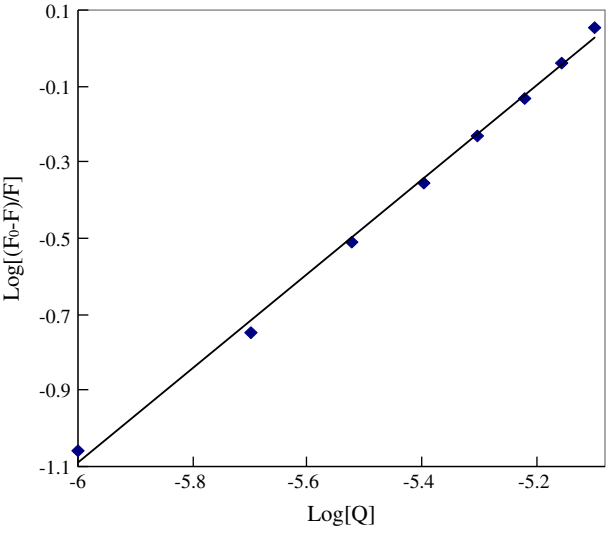

Figure 11. Plot of $\log[(F_0 - F)/F]$ *vs.* $\log[Q]$ for titration of the complex to BSA.

3.8.3. Binding constant and number of binding sites. In general, when small molecules bind independently to a set of equivalent sites on a macromolecule, the equilibrium between the free and bound molecule is given by the following equation [64, 65]:

$$\log[(F_0 - F)/F] = \log K + n \log[Q] \quad (5)$$

where F_0 and F represent the fluorescence intensities in the absence and presence of quencher, respectively. K is the binding constant of the dicopper(II) complex with BSA and n is the binding sites. From the quenching plot of $\log[(F_0 - \mathrm{F})/F]$ *versus* $\log[Q]$ (figure 11), the K and n values of the dicopper(II) complex obtained are $2.09 \times 10^6\,\mathrm{M}^{-1}$ and 1.23 for the dicopper(II) complex ($R = 0.9985$ for eight points).

4. Conclusions

To investigate the influence of structural variation of the bridging ligands in dicopper(II) complexes on DNA- and protein-binding properties as well as cytotoxic activities, a new dicopper(II) complex, $[Cu_2(oxbpa)(phen)(H_2O)](pic)\cdot 2H_2O$, has been synthesized and structurally characterized using *N*-benzoato-*N*′-(hydroxypropyl)oxamide (H_3oxbpa) as a bridging ligand and 1,10-phenanthroline. The reactivity towards HS-DNA and BSA as well as cytotoxic activities of the dicopper(II) complex are investigated, revealing that the dicopper(II) complex interacts with DNA by intercalation, and the complex binds to BSA responsible for the quenching of tryptophan fluorescence by static quenching mechanism. Comparing the DNA-binding properties with other polycopper(II) complexes with similar structures, it is obvious that the bridging ligands in these oxamido-bridged complexes influence the DNA-binding ability. The *in vitro* cytotoxic activities suggest that the dicopper(II) complex is active against selected tumor cell lines. Varying substituent groups on oxamido-bridges in dinuclear complexes result in the differences in the space configuration and the electron density, *in vitro* antitumor activities as well as their DNA-binding abilities. Thus the affinity magnitudes toward HS-DNA and cytotoxic activities may be controlled and tuned by the nature of the bridging ligands in dinuclear complexes, valuable in understanding DNA and protein-binding properties of the dinuclear complexes as well as laying a foundation for the design of powerful agents for probing and targeting nucleic acids and proteins.

Supplementary materials

Crystallographic data for the structural analysis of the complex has been deposited with the Cambridge Crystallographic Data Center, CCDC No. 909436. Copies of this information can be obtained free from The Director, CCDC, 12 Union Road, Cambridge, CB2 1EZ, UK (Fax: C44 1233 336 033; E-mail: deposit@ccdc.cam.ac.uk).

Acknowledgments

This project was supported by the National Natural Science Foundation of China (Nos. 21071133 51273184 and 81202399), the Program for Science and Technology of

Shandong Province (2011GHY11521), the Natural Science Foundation of Qingdao City (Nos. 11-2-4-1-(9)gch, 12-1-3-52-(1)-nsh and 12-1-4-16-(7)-jch), and the Open Research Fund Program of Key Laboratory of Marine Drugs (Ocean University of China), Ministry of Education (No. KLMD(OUC)201204).

References

[1] M. Chauhan, K. Banerjee, F. Arjmand. *Inorg. Chem.*, **46**, 3072 (2007).
[2] F. Arjmand, M. Aziz. *Eur. J. Med. Chem.*, **44**, 834 (2009).
[3] M.J. Clarke. *Coord. Chem. Rev.*, **236**, 209 (2003).
[4] T. Boulikas, M. Vougiouka. *Oncol. Rep.*, **10**, 1663 (2003).
[5] E. Wong, C.M. Giandomenico. *Chem. Rev.*, **99**, 2451 (1999).
[6] B. Rosenberg, L. Vancamp, J.E. Trosko, V.H. Mansour. *Nature*, **222**, 385 (1969).
[7] E.R. Jamieson, S.J. Lippard. *Chem. Rev.*, **99**, 2467 (1999).
[8] J. Tan, B. Wang, L. Zhu. *Bioorg. Med. Chem.*, **17**, 614 (2009).
[9] H. Xu, K.C. Zheng, Y. Chen, Y.Z. Li, L.J. Lin, H. Li, P.X. Zhang, L.N. Ji. *J. Chem. Soc. Dalton Trans.*, 2260 (2003).
[10] M. Asadi, E. Safaei, B. Ranjbar, L. Hasani. *New J. Chem.*, **28**, 1227 (2004).
[11] H. Malonga, J.F. Neault, H.A. Tajmir-Riahi. *DNA Cell Biol.*, **25**, 393 (2006).
[12] H. Gao, Y.N. Wang, Y.G. Fan, J.B. Ma. *Bioorg. Med. Chem.*, **14**, 131 (2006).
[13] Z.A. Siddiqi, M. Khalid, S. Kumar, M. Shahid, S. Noor. *Eur. J. Med. Chem.*, **45**, 264 (2010).
[14] D.R. Green, J.C. Reed. *Science*, **281**, 1309 (1998).
[15] Y. Ma, L. Cao, T. Kavabata, T. Yoshino, B.B. Yang, S. Okada. *Free Radical Biol. Med.*, **25**, 568 (1998).
[16] F. Liang, C. Wu, H. Lin, T. Li, D. Gao, Z. Li, J. Wei, C. Zheng, M. Sun. *Bioorg. Med. Chem. Lett.*, **13**, 2469 (2003).
[17] J. Easmon, G. Purstinger, G. Heinisch, T. Roth, H.H. Fiebig, W. Holzer, W. Jager, M. Jenny, J. Hofmann. *J. Med. Chem.*, **44**, 2164 (2001).
[18] E.L. Hegg, J.N. Burstyn. *Coord. Chem. Rev.*, **173**, 133 (1998).
[19] S. Dhar, D. Senapati, P.K. Das, P. Chattopadhyay, M. Nethaji, A.R. Chakravarty. *J. Am. Chem. Soc.*, **125**, 12118 (2003).
[20] S. Dhar, P.A. Reddy, M. Nethaji, S. Mahadevan, M.K. Saha, A.R. Chakravarty. *Inorg. Chem.*, **41**, 3469 (2002).
[21] D.S. Sigman, D.R. Graham, V.D. Aurora, A.M. Stern. *J. Biol. Chem.*, **254**, 12269 (1979).
[22] R. Rao, A.K. Patra, P.R. Chetana. *Polyhedron*, **27**, 1343 (2008).
[23] N. Raman, R. Jeyamurugan. *J. Coord. Chem.*, **62**, 2375 (2009).
[24] X. Wang, Y.T. Li, Z.Y. Wu, X.W. Li, C.W. Yan. *Struct. Chem.*, **23**, 1509 (2012).
[25] S. Anbu, M. Kandaswamy. *Polyhedron*, **30**, 123 (2011).
[26] J.Z. Wu, L. Yuan, J.F. Wu. *J. Inorg. Biochem.*, **99**, 2211 (2005).
[27] Z.D. Matovic, V.D. Miletic, G. Samardzic, G. Pelosi, S. Ianelli, S. Trifunovic. *Inorg. Chim. Acta*, **358**, 3135 (2005).
[28] S.H. Cui, M. Jiang, Y.T. Li, Z.Y. Wu, X.W. Li. *J. Coord. Chem.*, **23**, 4209 (2011).
[29] B.M. Ji, Z.X. Zhou, K.L. Ding, Y.Z. Li. *Polyhedron*, **17**, 4327 (1998).
[30] G.M. Sheldrick. *Acta Cryst.*, **A64**, 112 (2008).
[31] J. Marmur. *Mol. J. Biol.*, **3**, 208 (1961).
[32] M.E. Reichmann, S.A. Rice, C.A. Thomas, P.J. Doty. *J. Am. Chem. Soc.*, **76**, 3047 (1954).
[33] J.B. Chaires, N. Dattagupta, D.M. Crothers. *Biochemistry*, **21**, 3933 (1982).
[34] P.T. Selvi, H. Stoeckli-Evans, M. Palaniandavar. *J. Inorg. Biochem.*, **99**, 2110 (2005).
[35] G. Cohen, H. Eisenberg. *Biopolymers*, **8**, 45 (1969).
[36] J.K. Barton, J.M. Goldberg, C.V. Kumar, N.J. Turro. *J. Am. Chem. Soc.*, **108**, 2081 (1986).
[37] N.S. Quiming, R.B. Vergel, M.G. Nicolas. *Villanueva. J. Health Sci.*, **51**, 8 (2005).
[38] W.J. Geary. *Coord. Chem. Rev.*, **7**, 81 (1971).
[39] H. Ojima, K. Nonoyama. *Coord. Chem. Rev.*, **92**, 85 (1988).
[40] P. Siega, V. Vrdoljak, C. Tavagnacco, R. DreosInorg. *Inorg. Chim. Acta*, **387**, 93 (2012).
[41] A.W. Addison, T.N. Rao, J. Reedijk, J. VanRijin, G.C. Verschoor. *J. Chem. Soc., Dalton Trans*., 1349 (1984).
[42] A. Wolf, G.H. Shimer, T. Meehan. *Biochemistry*, **26**, 6392 (1987).
[43] J.B. LePecq, C. Paoletti. *J. Mol. Biol.*, **27**, 87 (1967).
[44] Y. Mei, J.J. Zhou, H. Zhou, Z.Q. Pan. *J. Coord. Chem.*, **65**, 643 (2012).
[45] H.L. Wu, X.C. Huang, B. Liu, F. Kou, F. Jia, J.K. Yuan, Y. Bai. *J. Coord. Chem.*, **64**, 4383 (2011).
[46] K. Pothiraj, T. Baskaran, N. Raman. *J. Coord. Chem.*, **65**, 2110 (2012).

[47] C.Y. Gao, X.F. Ma, J. Lu, Z.G. Wang, J.L. Tian, S.P. Yan. *J. Coord. Chem.*, **64**, 2157 (2011).
[48] M. Jiang, Y.T. Li, Z.Y. Wu. *J. Coord. Chem.*, **65**, 1858 (2012).
[49] F.J. Meyer-Almes, D. Porschke. *Biochemistry*, **32**, 4246 (1993).
[50] B.C. Baguley, M.L. Bret. *Biochemistry*, **23**, 937 (1984).
[51] R.F. Pasternack, M. Cacca, B. Keogh, T.A. Stephenson, A.P. Williams, E.J. Gibbs. *J. Am. Chem. Soc.*, **113**, 6835 (1991).
[52] S.S. Mazzefa, F. Bettio, M. Mozzon, R. Bertani, A. Venzo, F. Benetollo, R.A. Michelin, V. Gandin, C. Marzano. *J. Med. Chem.*, **50**, 4775 (2007).
[53] O. Stern, M. Volmer. *Z. Phys.*, **20**, 183 (1919).
[54] H.H. Lu, Y.T. Li, Z.Y. Wu, K. Zheng, C.W. Yan. *J. Coord. Chem.*, **64**, 1360 (2011).
[55] Y.J. Zheng, X.W. Li, Y.T. Li, Z.Y. Wu, C.W. Yan. *J. Coord. Chem.*, **65**, 3530 (2012).
[56] S. Mahadevan, M. Palaniandavar. *Inorg. Chem.*, **37**, 693 (1998).
[57] Y.M. Song, P.J. Yang, M.L. Yang, J.W. Kang, S.Q. Qin, B.Q. Lu. *Transition Met. Chem.*, **28**, 712 (2003).
[58] M.T. Carter, M. Rodriguez, A.J. Bard. *J. Am. Chem. Soc.*, **111**, 8901 (1989).
[59] S. Satyanarayana, J.C. Dabrowiak, J.B. Chaires. *Biochemistry*, **31**, 9319 (1992).
[60] L. Jin, P. Yang. *J. Inorg. Biochem.*, **68**, 79 (1997).
[61] Y.Y. Yue, X.G. Chen, J. Qin, X.J. Yao. *Dyes Pigm.*, **79**, 176 (2008).
[62] S.S. Bhat, A.A. Kumbhar, H. Heptullah, A.A. Khan, V.V. Gobre, S.P. Gejji, V.G. Puranik. *Inorg. Chem.*, **50**, 545 (2011).
[63] W.R. Ware. *J. Phys. Chem.*, **66**, 455 (1962).
[64] V. Anbazhagan, R. Renganathan. *J. Lumin.*, **128**, 1454 (2008).
[65] P. Banerjee, S. Ghosh, A. Sarkar, S.C. Bhattacharya. *J. Lumin.*, **131**, 316 (2011).